Human C-reactive protein slows atherosclerosis development in a mouse model with human-like hypercholesterolemia

Alexander Kovacs[†], Per Tornvall[‡], Roland Nilsson[§¶], Jesper Tegnér[§¶], Anders Hamsten[†‡], and Johan Björkegren[§‖]

[§]Computational Medicine Group, [†]Atherosclerosis Research Unit, Center for Molecular Medicine, Department of Medicine, and [‡]Cardiology Unit, Department of Medicine, Karolinska Institutet, Karolinska University Hospital, 171 76 Stockholm, Sweden; and [¶]Computational Biology Group, Department of Physics, Linköping Institute for Technology, Linköping University, 581 83 Linköping, Sweden

Communicated by Alexander G. Bearn, American Philosophical Society, Philadelphia, PA, June 30, 2007 (received for review May 1, 2007)

Increased baseline values of the acute-phase reactant C-reactive protein (CRP) are significantly associated with future cardiovascular disease, and some *in vitro* studies have claimed that human CRP (hCRP) has proatherogenic effects. *In vivo* studies in apolipoprotein E-deficient mouse models, however, have given conflicting results. We bred atherosclerosis-prone mice ($Apob^{100/100}Ldlr^{-/-}$), which have human-like hypercholesterolemia, with hCRP transgenic mice ($hCRP^{+/0}$) and studied lesion development at 15, 30, 40, and 50 weeks of age. Atherosclerotic lesions were smaller in $hCRP^{+/0}Apob^{100/100}Ldlr^{-/-}$ mice than in $hCRP^{0/0}Apob^{100/100}Ldlr^{-/-}$ controls, as judged from the lesion surface areas of pinned-out aortas from mice at 40 and 50 weeks of age. In lesions from 40-week-old mice, mRNA expression levels of several genes in the proteasome degradation pathway were higher in $hCRP^{+/0}Apob^{100/100}Ldlr^{-/-}$ mice than in littermate controls, as shown by global gene expression profiles. These results were confirmed by real-time PCR, which also indicated that the activities of those genes were the same at 30 and 40 weeks in $hCRP^{+/0}Apob^{100/100}Ldlr^{-/-}$ mice but were significantly lower at 40 weeks than at 30 weeks in controls. Our results show that hCRP is not proatherogenic but instead slows atherogenesis, possibly through proteasome-mediated protein degradation.

acute-phase protein | apolipoprotein B100 | coronary artery disease | low-density lipoprotein | plaques

The incidence of future cardiovascular disease events is greatly increased among individuals whose baseline values of serum C-reactive protein (CRP) are in the upper segment of the population distribution (1, 2), and *in vitro* studies suggest that human CRP (hCRP) may have a direct role in atherogenesis (3). To address this issue *in vivo*, atherosclerosis progression has been studied in apolipoprotein E knockout ($Apoe^{-/-}$) mice (4) cross-bred with transgenic mice expressing human (5, 6) or rabbit CRP (7). However, the results have been inconsistent. In one study, lesions developed faster in male *hCRP* transgenic mice on an $Apoe^{-/-}$ background than in nontransgenic $Apoe^{-/-}$ controls (6), but two other studies saw no effect of hCRP on atherogenesis in $Apoe^{-/-}$ mice (5, 7), and one study in *APOE**3-Leiden mice was also negative (8). The authors of the latter study noted that high levels of hCRP expression in mice are not physiological and that the results should be interpreted with caution (5, 7). In a subsequent report, atherosclerosis progression was accelerated or decelerated in $Apoe^{-/-}$ mice, depending on whether they were treated with native or modified forms of hCRP (9).

$Apoe^{-/-}$ mice have far more severe hypercholesterolemia than humans, and most of their cholesterol is contained in very low-density lipoproteins rather than in low-density lipoproteins (LDLs) as in humans. Furthermore, $Apoe^{-/-}$ mice are in a continuous state of low-grade systemic inflammation (10), and the apoE protein *per se* can alter immune responses (11). Thus, the $Apoe^{-/-}$ mouse model may not be ideal for studies of hCRP in atherosclerosis.

In this study, we investigated the effects of hCRP on lesion development in an atherosclerosis-prone mouse model with human-like hypercholesterolemia. To create this model, we bred hCRP transgenic mice (12) with LDL receptor-null mice that exclusively express apolipoprotein B100 (apoB100) ($Ldlr^{-/-}Apob^{100/100}$) (13) and analyzed lesion progression at 15, 30, 40, and 50 weeks in $CRP^{+/0}Ldlr^{-/-}Apob^{100/100}$ mice and littermate controls lacking CRP expression.

Results

Basic Characteristics. Except for plasma levels of hCRP, the basic characteristics of the $CRP^{+/0}Ldlr^{-/-}Apob^{100/100}$ mice did not differ from those of littermate controls at any time point (Table 1). Weight increased in both groups between weeks 15 and 30. Plasma cholesterol, triglyceride, and glucose levels were stable in both groups except for a statistically nonsignificant peak at 40 weeks. Importantly, both groups had similar serum amyloid A protein (SAA) levels, which increased in both groups until week 40 and then remained stable or decreased slightly at 50 weeks. Transgenic expression of hCRP thus did not have proinflammatory effects that triggered a response by this extremely sensitive acute-phase reactant. As expected, hCRP was only detected in $CRP^{+/0}Ldlr^{-/-}Apob^{100/100}$ mice. The median serum hCRP level was 24.0 mg/liter at 15 weeks and peaked at 51.8 mg/liter at 30 weeks ($P < 0.003$) (Table 1).

Atherosclerosis Development. Only occasional atherosclerotic lesions were observed in 15-week-old mice (Fig. 1*A*). At 30 weeks, both focal plaques (deep red with distinct boundaries) and fatty lesions (light red with no distinct boundaries) were present in the aortic arch of both $CRP^{+/0}Ldlr^{-/-}Apob^{100/100}$ mice and controls. Scattered fatty lesions were also found in the abdominal region. At 40 weeks, however, the lesions were significantly larger in the controls ($P = 0.027$) (Fig. 1*B*), and only the controls had plaques in the abdominal aorta, reflecting further expansion of the lesions. In CRP-positive mice, the mean lesion size did not increase between 30 and 40 weeks. At 50 weeks, the extent of plaques had increased in both groups (Fig. 1*B*). In $CRP^{+/0}Ldlr^{-/-}Apob^{100/100}$ mice, the lesion surface area increased to approximately the same level as in controls at 40 weeks. In the controls,

Author contributions: A.K., P.T., A.H., and J.B. designed research; A.K. and J.B. performed research; A.K., R.N., J.T., and J.B. analyzed data; and A.K. and J.B. wrote the paper.

The authors declare no conflict of interest.

Abbreviations: CRP, C-reactive protein; hCRP, human CRP; LDL, low-density lipoprotein; apoB100, apolipoprotein B100; SAA, serum amyloid A; C3, complement component 3; LFDR, local false discovery rate.

[‖]To whom correspondence should be addressed at: Computational Medicine Group, Atherosclerosis Research Unit, King Gustaf V Research Institute, Karolinska Institutet, Karolinska Hospital, 171 76 Stockholm, Sweden. E-mail: johan.bjorkegren@ki.se.

This article contains supporting information online at www.pnas.org/cgi/content/full/0706027104/DC1.

Table 1. Characteristics of *Ldlr*$^{-/-}$*Apob*$^{100/100}$ mice with and without hCRP expression

	15 weeks		30 weeks		40 weeks		50 weeks	
Variable	CRP$^{+/0}$ (n = 7)	CRP$^{0/0}$ (n = 6)	CRP$^{+/0}$ (n = 24)	CRP$^{0/0}$ (n = 19)	CRP$^{+/0}$ (n = 12)	CRP$^{0/0}$ (n = 10)	CRP$^{+/0}$ (n = 12)	CRP$^{0/0}$ (n = 15)
Weight	26.3 ± 2.4	23.0 ± 1.5	33.0 ± 4.5	32.3 ± 3.7	35.0 ± 7.7	34.8 ± 6.3	35.2 ± 5.5	34.9 ± 5.6
Cholesterol	343 ± 3	330 ± 37	330 ± 55	308 ± 57	375 ± 150	356 ± 127	330 ± 41	377 ± 92
Triglycerides	134 ± 12	124 ± 11	147 ± 31	137 ± 25	199 ± 57	168 ± 66	137 ± 39	155 ± 61
Glucose	230 ± 104	142 ± 20	374 ± 96	399 ± 76	544 ± 177	541 ± 157	366 ± 109	375 ± 107
SAA	3.6 (2.8–11.3)	6.0 (3.8–6.7)	4.8 (1.5–19.9)	1.9 (1.7–3.6)	10.5 (1.2–27.5)	34.3 (0.8–95.4)	2.2 (0.4–54.9)	8.3 (3–60.3)
CRP	24.0 (22.5–33.5)	0 (0)	51.8 (45.1–59.2)	0 (0)	37.0 (28.6–59.3)	0 (0)	41.7 (38.7–53.3)	0 (0)

Values are mean ± SD and median (25th to 75th percentiles) in parentheses for SAA and CRP. There were no significant differences between the groups (CRP$^{+/0}$ vs. CRP$^{0/0}$) or within the groups between time points except for CRP, $P < 0.003$.

lesion expanded further and remained significantly larger than in *CRP*$^{+/0}$*Ldlr*$^{-/-}$*Apob*$^{100/100}$ mice ($P = 0.041$) (Fig. 1*B*). In summary, the extent of the lesions differed in the two groups ($P < 0.001$), and atherosclerosis development was delayed in hCPR-positive mice.

Lesion Histology and hCRP mRNA. As expected, hCRP was detected only in lesions from *CRP*$^{+/0}$*Ldlr*$^{-/-}$*Apob*$^{100/100}$ mice. hCRP could not be detected at 15 weeks but was clearly visible at 30 weeks, increased markedly at 40 weeks, and remained stable or decreased slightly at 50 weeks (Fig. 2*A*). The protein pattern was in accordance with hCRP mRNA levels at 30 and 40 weeks (data not shown). Complement component 3 (C3) followed a similar pattern in both groups, except that the staining was more focal in the controls. In both groups, CD68 staining was occasionally detected in 15-week lesions and then increased with lesion size over time; the extent of staining did not differ between groups (Fig. 2*A*). The same pattern was observed for Oil Red O and collagen staining (Fig. 2*B*), except that the area of collagen staining was ≈10% larger in *CRP*$^{+/0}$*Ldlr*$^{-/-}$*Apob*$^{100/100}$ mice than in controls at 50 weeks ($n = 5$ per group; $P < 0.05$).

Global Gene Expression and RT-PCR Validation. To identify differences in lesion mRNA levels that could explain the slower plaque development in *hCRP*$^{+/0}$*Apob*$^{100/100}$*Ldlr*$^{-/-}$ mice, we performed microarray studies in four mice from each group by using Mouse Genome 430 2.0 GeneChips (Affymetrix, Santa Clara, CA). Seven hundred forty-two differentially expressed atherosclerosis genes were identified [local false discovery rate (LFDR) <0.25 or uncorrected $P \approx 0.02$]. Gene Ontology analysis of these genes

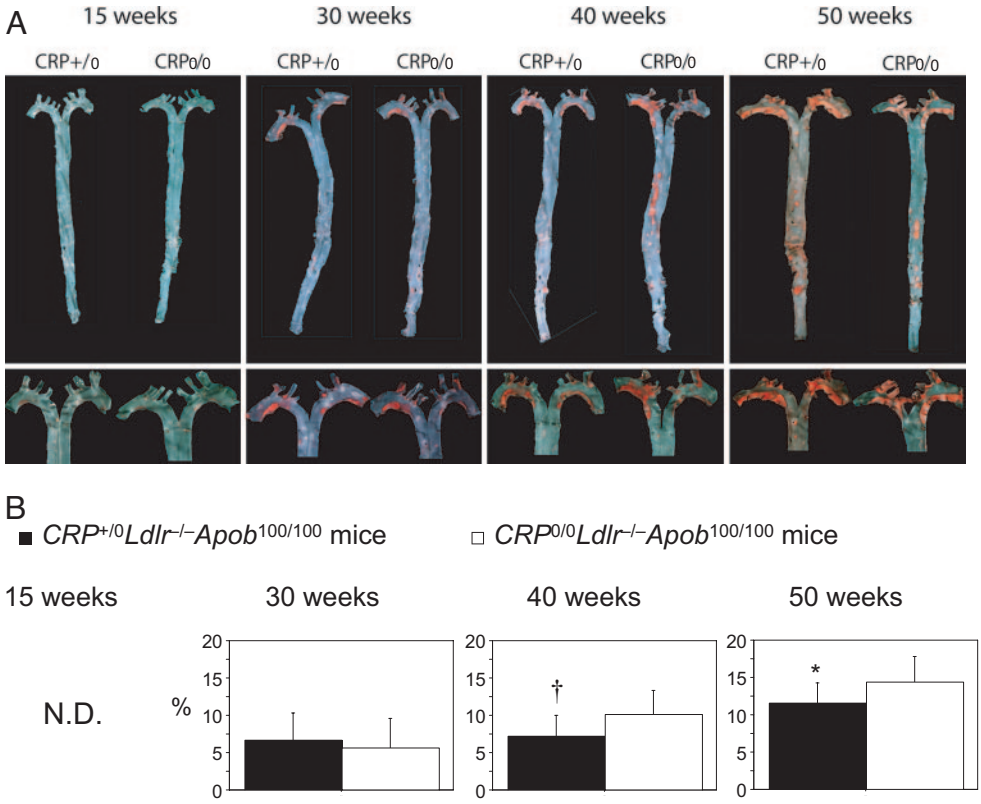

Fig. 1. Atherosclerosis development in *LDlr*$^{-/-}$*Apob*$^{100/100}$ mice with and without hCRP expression. (*A*) Sudan IV-stained atherosclerotic lesions in pinned-out aortas (*Upper*) and aortic arches of the same aortas (*Lower*) from representative mice in both groups. (*B*) Lesion surface area is reported as the area of Sudan IV staining, expressed as percentage of the entire surface area of the aorta from the iliac bifurcation to the aortic root. $n = 17$ *CRP*$^{+/0}$*Ldlr*$^{-/-}$*Apob*$^{100/100}$ mice (filled bars) and 19 controls (open bars) at 30 weeks; $n = 13$ and 10 at 40 weeks; $n = 11$ and 15 at 50 weeks. Values are mean ± SD. †, $P = 0.027$ (40 weeks); *, $P = 0.041$ (50 weeks) vs. control mice. N.D., not detectable.

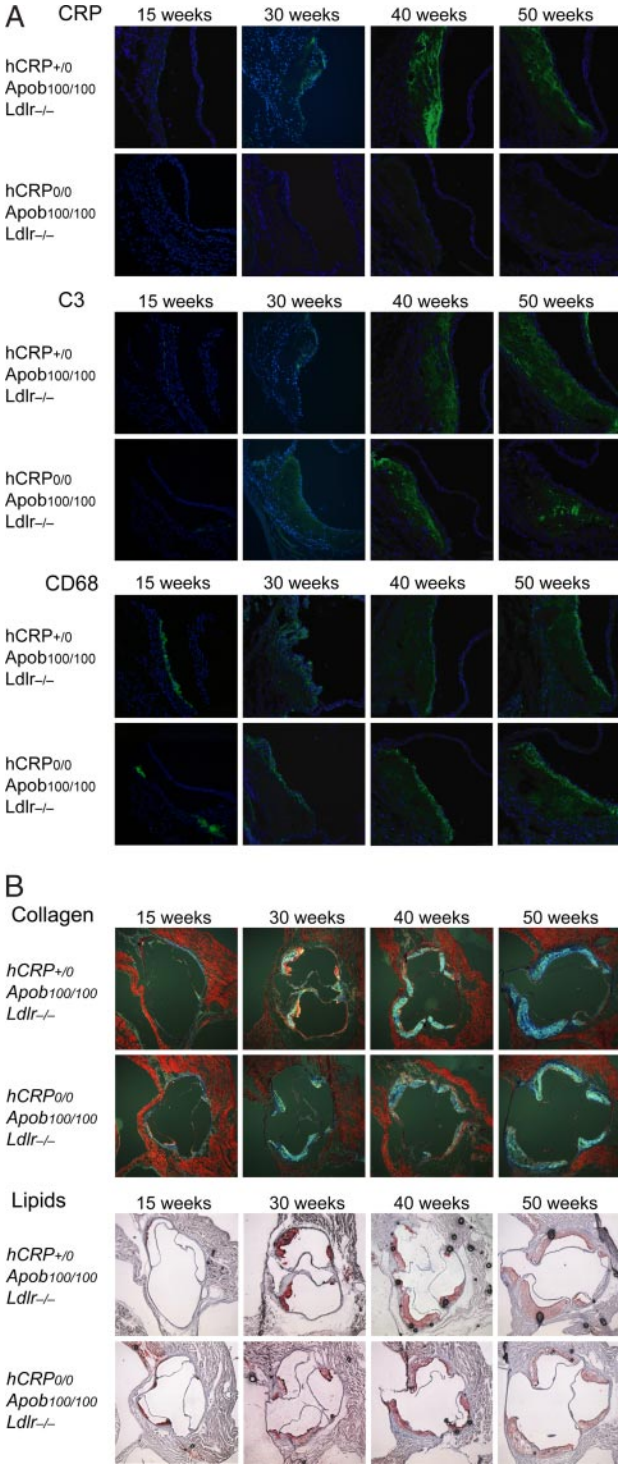

Fig. 2. Atherosclerosis histology of $Ldlr^{-/-}Apob^{100/100}$ mice with and without hCRP expression. (*A*) Immunofluorescence staining for CRP, C3, and CD68 in aortic root sections from $CRP^{+/0}Ldlr^{-/-}Apob^{100/100}$ mice and $CRP^{0/0}Ldlr^{-/-}Apob^{100/100}$ controls. Sections were incubated with primary antibodies and then with fluorescently labeled anti-rat IgG and counterstained with DAPI. (*B*) Aortic root sections stained with Masson's trichrome (collagen) and Oil Red O (lipids) from representative mice in both groups. Except for focal C3 staining in controls at 40 and 50 weeks and ≈10% more collagen in lesions of $CRP^{+/0}Ldlr^{-/-}Apob^{100/100}$ at 50 weeks ($n = 5 + 5$; $P < 0.05$), there were no other differences between groups.

(Fig. 3A) using DAVID software (http://david.abcc.ncifcrf.gov) revealed significant activity in the biological processes "protein catabolism" ($P = 1.81 \times 10^{-5}$), "cellular macromolecule catabolism" ($P = 5.23 \times 10^{-6}$), and "biopolymer catabolism" ($P = 1.12 \times 10^{-5}$); in the molecular functions "proteasome endopeptidase activity" ($P = 4.48 \times 10^{-15}$); and in the cellular components "proteasome core complex" ($P = 8.34 \times 10^{-15}$). These findings, together with the KEGG pathway analysis ("proteasome"; $P = 3.91 \times 10^{-15}$), strongly indicated that the altered activity in the proteasome degradation pathway was central. Gene set enrichment analysis, a statistical approach that, unlike Gene Ontology analysis, considers the entire GeneChip dataset [supporting information (SI) *Appendix 1*] rather than the differentially expressed genes only (LFDR < 0.25), was used for validation. The gene set enrichment analysis revealed that mRNA levels of the genes in the proteasome degradation pathway were consistently higher in $hCRP^{+/0}Ldlr^{-/-}Apob^{100/100}$ mice than in controls (Fig. 3*B*).

To validate the gene expression changes identified by GeneChip analysis, we used real-time PCR to examine mRNA from atherosclerotic lesions in 13 $hCRP^{+/0}Ldlr^{-/-}Apob^{100/100}$ (30 weeks, $n = 5$; 40 weeks, $n = 8$) and 15 littermate controls (30 weeks, $n = 7$; 40 weeks, $n = 8$). Specifically, we examined six genes encoding proteins central to proteasome degradation: the 20s proteasome subunits PSMA7, PSMB7, and PSMB9 (immunoproteasome subunit), the 19s proteasome cap unit PSMC6, the 11s proteasome cap unit PSME2, and E2 ubiquitin ligase (UBE2D3). Between 30 and 40 weeks, the mRNA levels of those genes were stable in $CRP^{+/0}Ldlr^{-/-}Apob^{100/100}$ mice but decreased significantly in controls (Fig. 3*C*). The levels were similar at 30 weeks in both groups ($P > 0.22$ for all genes). At 40 weeks, however, the levels were 1.3- to 2-fold higher in $CRP^{+/0}Ldlr^{-/-}Apob^{100/100}$ than in controls (PSME2, $P = 0.04$; PSMB7, $P = 0.053$; PSMA7, $P = 0.066$; PSMB9, $P = 0.074$; PSMC6, $P = 0.08$; Ube2D3, $P = 0.12$), reaching borderline significance.

Discussion

This study shows that transgenic expression of hCRP slows lesion progression in an atherosclerosis-prone mouse model with human-like hypercholesterolemia. Thus, hCRP was not proatherogenic but appeared to be atheroprotective. The slower progression was not associated with major changes in lesion histology; however, as the lesions expanded in mice lacking *hCRP*, the activity of several genes in the proteasome degradation pathway decreased, as judged by mRNA levels. Whether the proteasome degradation activity level is coupled to the presence of hCRP in the lesion and whether it slows atherosclerosis development remain to be shown.

Previous studies of CRP in atherogenesis in mice have been inconclusive. For instance, the atherosclerotic lesion area in $Apoe^{-/-}$ mice, as determined by Oil Red O staining of aortic root sections, was larger in *hCRP* transgenic mice than in controls (6). In contrast, two other studies of $Apoe^{-/-}$ mice (5, 7) and one of *APOE*3-Leiden* mice (8) did not detect a difference in the lesion area in the aortic root. Similarly, we could not detect a difference in the lesion area in aortic root sections in $CRP^{+/0}Ldlr^{-/-}Apob^{100/100}$ mice and controls. However, lesion areas in the entire aortic tree expanded more slowly in $CRP^{+/0}Ldlr^{-/-}Apob^{100/100}$ mice than in nontransgenic controls, as judged by *en face* analysis. In contrast, a previous *en face* analysis of $CRP^{+/0}Apoe^{-/-}$ mice showed that hCRP accelerated lesion expansion in the aortic tree (6).

These conflicting results suggest that the effects of CRP in atherosclerosis are dependent on the mouse model used. In support of this notion, $Apoe^{-/-}$ mice have altered immune responses that may directly involve apoE, including phagocytosis of apoptotic bodies, altered macrophage dynamics (10), and altered antigen presentation efficiency (15). Also, the effects of CRP on lesion development may be influenced by differences in the degree and type of lipoproteinemia in the mouse models. For instance, hCRP has a binding preference for LDLs rather than

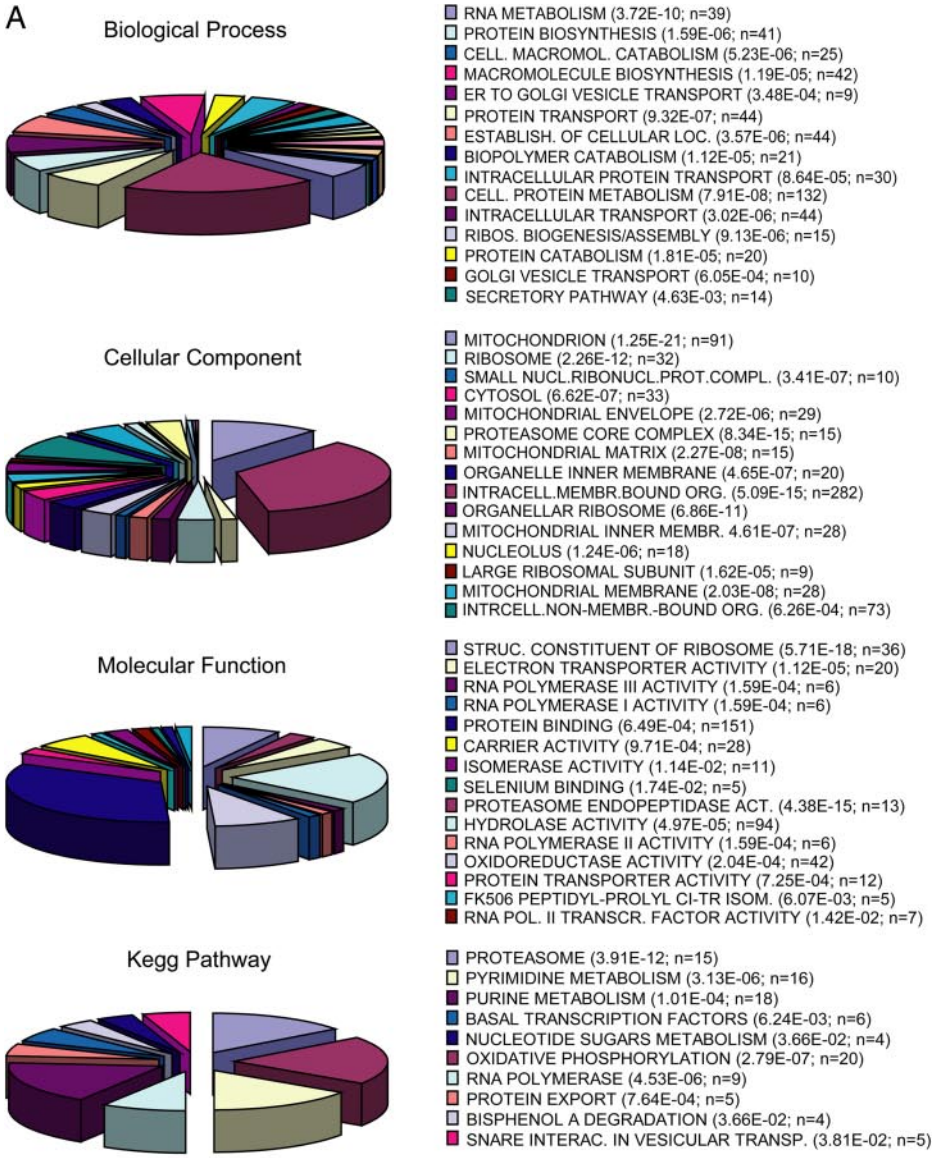

Fig. 3. Global gene expression analysis and real-time PCR of mRNA isolated from the arterial wall in the aortic arch, including the atherosclerotic lesions (see *Materials and Methods*) of mice at 30 and 40 weeks of age. (*A*) Pie charts of Gene Ontology categories (biological processes, molecular functions, and cellular component) and Kegg pathways generated from 742 differentially expressed genes (LFDR < 0.25; SI Table 2). The *P* values next to each category were calculated with Fisher's exact probability test (*SI Appendix 1*). (*B*) Heat map showing mRNA levels (blue, low; red, high) of genes (rows) in the proteasome degradation pathway, which was highly active in the $CRP^{+/0}Ldlr^{-/-}Apob^{100/100}$ mice compared with the controls (LFDR < 0.09), as shown by gene set enrichment analysis of the same GeneChips. Gene names marked in green were chosen for real-time PCR analysis. (*C*) mRNA levels of six genes central to proteasome degradation (PSMA7, PSMB7, PSMB9, PSMC6, PSME2, and UBE2D3) determined by real-time PCR of total RNA from aortic arch lesions in $CRP^{+/0}Ldlr^{-/-}Apob^{100/100}$ mice (filled bars) and $CRP^{-/-}Ldlr^{-/-}Apob^{100/100}$ controls (open bars) at 30 weeks ($n = 5$ and $n = 7$, respectively) and 40 weeks ($n = 8$ per group). Values are mean ± SD. *, $P < 0.02$; †, $P < 0.006$; ‡, $P < 0.02$; §, $P < 0.05$; ‖, $P < 0.006$; #, $P < 0.004$ vs. controls at 30 weeks.

very low-density lipoproteins (16). Thus, the atheroprotective role of hCRP we observed may be masked in $Apoe^{-/-}$ mice because they are very low-density lipoprotein animals and have altered immune functions.

In our study, collagen was slightly more abundant in the lesions of $CRP^{+/0}Ldlr^{-/-}Apob^{100/100}$ mice than in controls at 50 weeks, consistent with the findings of Paul *et al.* (6) in CRP transgenic mice. The CRP mice in that study also had increases in C3 deposits and macrophages (i.e., CD68). However, in our study, neither C3 deposits nor CD68 staining of lesions differed in $CRP^{+/0}Ldlr^{-/-}Apob^{100/100}$ mice and controls, although the C3 deposits appeared to be more focal in controls at 40 weeks and even more so at 50 weeks (Fig. 2). In the only other mouse study of CRP in relation to atherogenesis in which C3 was investigated, Hirschfield *et al.* (5) showed no difference in lesion C3 deposits or in CD68 staining. We also detected hCRP protein in the lesions of $CRP^{+/0}Ldlr^{-/-}Apob^{100/100}$ mice, as did Paul *et al.* (6) and Hirschfield *et al.* (5) in their CRP transgenic mice; however, Trion *et al.* (8) did not. In addition, we detected *hCRP* mRNA in the plaques of our CRP transgenic mice but not in controls.

The slower development of atherosclerosis in our *hCRP* transgenic mice may be explained, at least in part, by persistently high levels of proteasome activity. hCRP binds to modified LDL and could thereby promote its uptake by cells and clearance from the plaques (17, 18). The proteasome degradation pathway is a central component of the ubiquitin proteasome system, which degrades oxidized and misfolded proteins in the cell (19, 20) and regulates pathways of inflammation, cell proliferation, and apoptosis (20). In a recent study of carotid plaques, decreased proteasome activity was a hallmark of patients with cerebral symptoms, and the activity was lowest in patients who had already suffered a stroke (21). Decreased proteasome degradation activity has also been implicated in immunopresentation to T cells via the MHC-I pathway. It was thought that immunopresentation via this pathway was mainly restricted to intracellular proteins, but recent data strongly support cross-presentation between the MHC-I and MHC-II pathways, in which proteins are delivered to the proteasomes by endocytosis (22, 23). Interestingly, the transport protein SEC61, which is thought to facilitate cross-presentation, was highly up-regulated in CRP transgenic mice (24). It should be noted that the observed differences in mRNA levels of lesion proteasomes between the study groups could, alternatively to actual gene expression differences, be a consequence of differences in plaque burden and/or cellular composition of the plaque.

In summary, by using an atherosclerosis-prone mouse model with human-like hypercholesterolemia, we show that human CRP is antiatherogenic, not proatherogenic, and slows the development of atherosclerosis.

Materials and Methods

Study Mice. The $Ldlr^{-/-}Apob^{100/100}$ mouse model has a plasma lipoprotein profile similar to that of familial hypercholesterolemia, which causes rapid progression of atherosclerosis (25). Mice transgenic for a 31-kb Cla fragment of *hCRP* ($CRP^{+/0}$100% C57BL/6) (12) were crossed with male $Ldlr^{-/-}Apob^{100/100}$ mice (≈6.25% 129/SvJae, ≈93.75% C57BL/6) to generate $CRP^{+/0}Ldlr^{-/-}Apob^{100/100}$ mice and littermate $CRP^{0/0}Ldlr^{-/-}Apob^{100/100}$ controls (>97% C57BL/6). Males were used for the study and housed four to six per cage, subjected to a 12-hour light/12-h dark cycle, and fed a chow diet ad libitum. Plasma samples were obtained and the mice were weighed every 10 weeks throughout the study. Plasma cholesterol and triglyceride concentrations were determined with colorimetric assays (INFINITY cholesterol/triglyceride kits; Thermo Trace, Noble Park, Victoria, Australia) and glucose levels with Precision Xtra (MediScience, Medford, MA). SAA and CRP were measured by ELISA [BioSource (Camarillo, CA) and Haemochrom (Essen, Germany), respectively]. Mouse genotypes were determined by PCR. The study was approved by the local ethics committee.

***En Face* Analysis and Histology.** Aortas were pinned out flat on a black wax surface as described (26), stained with Sudan IV, photographed with a Nikon (Melville, NY) SMZ1000 microscope, and analyzed with Easy Image Analysis 2000 software (Tekno Optik, Huddinge, Sweden). Lesion area was calculated as a percentage of the entire aortic surface between the aortic root and the iliac bifurcation. Aortic roots were isolated, immediately frozen in liquid nitrogen, and embedded in OCT compound (Histolab, Göteborg, Sweden). Randomly selected cryosections (10 μm) isolated between 100 and 800 μm distal to the cusps were stained with Oil Red O or Masson's trichrome (Sigma-Aldrich, St. Louis, MO) as described (27). In parallel, another set of randomly selected sections was sequentially incubated for 10 min in cold acetone, for 30 min in sodium borhydride to quench autofluorescence, and finally for 30 min in 0.2% Tween/PBS. Then, the sections were incubated with primary rat anti-mouse antibodies against CD68 (Serotec, Raleigh, NC), C3 (Abcam, Cambridge, MA), and CRP (Sigma-Aldrich) overnight at 4°C, with fluorescently labeled anti-rat IgG (Vector Laboratories, Burlingame, CA) to detect the primary antibody, and counterstained in mounting medium containing DAPI (Vector Laboratories). Fluorescently labeled slides were scanned with a Zeiss confocal microscope (Carl Zeiss, Oberkochen, Germany) at ×20 magnification. Slides stained with Masson's trichrome were scanned with a Leica fluorescence microscope (Leica Microsystems, Wetzlar, Germany) at ×10 magnification using brightfield settings. Areas positive for Masson's trichrome were measured with Easy Image Analysis 2000 software. Five replicates with 100-μm separation were used for all experiments.

RNA Isolation and GeneChip Analysis. Aortas were perfused with RNAlater (Qiagen, Valencia, CA), and the thoracic aorta from the third rib to the aortic root was carefully dissected and homogenized with FastPrep (Qbiogene, Montreal, Canada). Total RNA was isolated with RNeasy Mini Kits (Qiagen) including a DNase I treatment step. RNA quality was assessed with a Bioanalyzer 2100 (Agilent, Palo Alto, CA). High-quality RNA samples from four $CRP^{+/0}Ldlr^{-/-}Apob^{100/100}$ and four littermate controls were used for expression analyses with Mouse Genome 430 2.0 GeneChips (Affymetrix). All samples were prepared with the two-cycle protocol recommended by the manufacturer. Arrays were scanned with GeneChip Scanner 3000 and analyzed with GeneChip Operating Software (Affymetrix).

Real-Time PCR. Total RNA (0.3 μg) was reverse transcribed with SuperScript II according to the manufacturer's protocol (Invitrogen, Carlsbad, CA). After dilution of the cDNA to 65 μl, 3 μl of cDNA were amplified by real-time PCR with 1× *Taq*Man universal PCR master mix (Applied Biosystems, Foster City, CA). Assay-on-Demand kits containing primers and probes for hCRP (Hs00357041_m1), PSMA7 (Mm00478829_m1), PSMB7 (Mm01327044_m1), PSMB9 (Mm00479004_m1), PSMC6 (Mm00458820_m1), PSME2 (Mm01702833_g1), Ube2D3 (Mm01318861_m1), and the housekeeping genes ARBP (Mm00725448_s1) and cyclophilin A (forward, GGCCGATGACGAGCCC; reverse, GTCTTTGGAACTTTGTCTGCAA; probe, TGGGCCGCGTCTCCTTCGA) were from Applied Biosystems.

Statistical Analysis. Differences in normally distributed parameters such as the mRNA levels of selected genes, plasma measurements, and lesion surface areas between time points/

genotypes, were analyzed with unpaired *t* tests. Nonparametric tests (Kruskal–Wallis) were used for plasma CRP and SAA. Microarray data were normalized at the probe level with the quantile normalization method (28). Signal-level data were computed with the robust multichip average method (29) for 16,607 probe sets constructed by sequence matching against Refseq NM transcripts, as described (30). The data were log-transformed, and differential expression was assessed with the regularized *t* statistic (31). LFDRs were computed with the empirical Bayes method of Efron *et al.* (31). All analyses were implemented in Mathematica 5.1 (Wolfram Research, Champaign, IL). DAVID software was used to assess Gene Ontology and Kegg pathways (see also *SI Appendix 1*). Gene set enrichment analysis (*SI Appendix 1*) (14, 32) was performed as an independent test of the empirical Bayes method.

We received the hCRP-transgenic mice from Prof. Bruno Kyewski (National Center for Tumor Diseases, Heidelberg, Germany). This work was supported by grants from the Swedish Research Council (to J.B.), the Swedish Heart–Lung Foundation (to J.B.), The King Gustaf V and Queen Victoria Foundation (to J.B.), the Karolinska Institutet (to J.B. and A.H.), the Stockholm County Council (to J.B. and A.H.), the Swedish Society of Medicine (to J.B. and J.T.), The Hans and Loo Osterman Foundation for Geriatric Research (to J.B.), The Professor Nanna Swartz Fund (to J.B.), the Foundation for Old Servants (to J.B.), The Magnus Bergvalls Foundation (to J.B.), Åke Wiberg Stiftelse (to J.B.), and by an independent research grant from Pfizer Sweden AB (to J.B., P.T., and A.H.).

1. Danesh J, Wheeler JG, Hirschfield GM, Eda S, Eiriksdottir G, Rumley A, Lowe GD, Pepys MB, Gudnason V (2004) *N Engl J Med* 350:1387–1397.
2. Ridker PM, Wilson PWF, Grundy SM (2004) *Circulation* 109:2818–2825.
3. Jialal I, Devaraj S, Venugopal SK (2004) *Hypertension* 44:6–11.
4. Plump AS, Smith JD, Hayek T, Aalto-Setala K, Walsh A, Verstuyft JG, Rubin EM, Breslow JL (1992) *Cell* 71:343–353.
5. Hirschfield GM, Gallimore JR, Kahan MC, Hutchinson WL, Sabin CA, Benson GM, Dhillon AP, Tennent GA, Pepys MB (2005) *Proc Natl Acad Sci USA* 102:8309–8314.
6. Paul A, Ko KW, Li L, Yechoor V, McCrory MA, Szalai AJ, Chan L (2004) *Circulation* 109:647–655.
7. Reifenberg K, Lehr HA, Baskal D, Wiese E, Schaefer SC, Black S, Samols D, Torzewski M, Lackner KJ, Husmann M, *et al.* (2005) *Arterioscler Thromb Vasc Biol* 25:1641–1646.
8. Trion A, de Maat MP, Jukema JW, van der Laarse A, Maas MC, Offerman EH, Havekes LM, Szalai AJ, Princen HM, Emeis JJ (2005) *Arterioscler Thromb Vasc Biol* 25:1635–1640.
9. Schwedler SB, Amann K, Wernicke K, Krebs A, Nauck M, Wanner C, Potempa LA, Galle J (2005) *Circulation* 112:1016–1023.
10. Grainger DJ, Reckless J, McKilligin E (2004) *J Immunol* 173:6366–6375.
11. Laskowitz DT, Lee DM, Schmechel D, Staats HF (2000) *J Lipid Res* 41:613–620.
12. Murphy C, Beckers J, Ruther U (1995) *J Biol Chem* 270:704–708.
13. Farese RV, Jr, Veniant MM, Cham CM, Flynn LM, Pierotti V, Loring JF, Traber M, Ruland S, Stokowski RS, Huszar D, *et al.* (1996) *Proc Natl Acad Sci USA* 93:6393–6638.
14. Subramanian A, Tamayo P, Mootha VK, Mukherjee S, Ebert BL, Gillette MA, Paulovich A, Pomeroy SL, Golub TR, Lander ES, *et al.* (2005) *Proc Natl Acad Sci USA* 102:15545–15550.
15. Tenger C, Zhou X (2003) *Immunology* 109:392–397.
16. de Beer FC, Soutar AK, Baltz ML, Trayner IM, Feinstein A, Pepys MB (1982) *J Exp Med* 156:230–242.
17. Bhakdi S, Dorweiler B, Kirchmann R, Torzewski J, Weise E, Tranum-Jensen J, Walev I, Wieland E (1995) *J Exp Med* 182:1959–1971.
18. Bhakdi S, Torzewski M, Paprotka K, Schmitt S, Barsoom H, Suriyaphol P, Han SR, Lackner KJ, Husmann M (2004) *Circulation* 109:1870–1876.
19. Vieira O, Escargueil-Blanc I, Jurgens G, Borner C, Almeida L, Salvayre R, Negre-Salvayre A (2000) *FASEB J* 14:532–542.
20. Herrmann J, Ciechanover A, Lerman LO, Lerman A (2004) *Cardiovasc Res* 61:11–21.
21. Versari D, Herrmann J, Gossl M, Mannheim D, Sattler K, Meyer FB, Lerman LO, Lerman A (2006) *Arterioscler Thromb Vasc Biol* 26:2132–2139.
22. Wilson NS, Villadangos JA (2005) *Adv Immunol* 86:241–305.
23. Stow JL, Manderson AP, Murray RZ (2006) *Nat Rev Immunol* 6:919–929.
24. Bird L (2006) *Nat Rev Immunol* 6:880–881.
25. Lieu HD, Withycombe SK, Walker Q, Rong JX, Walzem RL, Wong JS, Hamilton RL, Fisher EA, Young SG (2003) *Circulation* 107:1315–1321.
26. Veniant MM, Sullivan MA, Kim SK, Ambroziak P, Chu A, Wilson MD, Hellerstein MK, Rudel LL, Walzem RL, Young SG (2000) *J Clin Invest* 106:1501–1510.
27. Stotz E, Schenk EA, Churukian C, Willis C (1986) *Stain Technol* 61:187–190.
28. Bolstad BM, Irizarry RA, Astrand M, Speed TP (2003) *Bioinformatics* 19:185–193.
29. Irizarry RA, Bolstad BM, Collin F, Cope LM, Hobbs B, Speed TP (2003) *Nucleic Acids Res* 31:e15.
30. Mecham BH, Klus GT, Strovel J, Augustus M, Byrne D, Bozso P, Wetmore DZ, Mariani TJ, Kohane IS, Szallasi Z (2004) *Nucleic Acids Res* 32:e74.
31. Efron B, Tibshirani R, Storey J, Tusher V (2001) *J Am Stat Assoc* 96:1151–1160.
32. Mootha VK, Lindgren CM, Eriksson KF, Subramanian A, Sihag S, Lehar J, Puigserver P, Carlsson E, Ridderstrale M, Laurila E, *et al.* (2003) *Nat Genet* 34:267–273.